Friction Control in Automotive Seat Belt Systems by Piezoelectrically Generated Ultrasonic Vibrations

Shravan Bharadwaj, Marcelo J. Dapino

Smart Vehicle Concept Center, Department of Mechanical Engineering,
The Ohio State University, Columbus, OH 43210, USA

ABSTRACT

Active control of friction between sliding surfaces is of significant interest in automotive applications. It has been shown that the friction force between sliding surfaces can be reduced by superimposing ultrasonic vibrations on the sliding velocity. This principle can be applied to systems in which solid state lubrication is advantageous. This paper investigates ultrasonic lubrication for creating adaptive seat belts with controllable force at the interface between the D-ring and webbing. By precisely controlling the seat belt force during a crash event, superior restraint can be achieved relative to existing systems which are designed as a compromise for various occupants and loading conditions. Proof-of-concept experiments are conducted in order to experimentally determine the performance limits and mechanics of a seat belt webbing subjected to macroscopic sliding motion and superimposed out-of-plane ultrasonic vibrations. The experimental setup consists of a high-capacity ultrasonic plastic welder and an apparatus for creating controlled relative motion between the welder tip and seat belt webbing. Analytical modeling using LuGre friction is presented which characterizes the parametric dependence of friction reduction on system settings in the presence of ultrasonic vibrations.

Keywords: Ultrasonic lubrication, adaptive seat belts, LuGre model

1. INTRODUCTION

Friction can be defined as the resistance to motion experienced when two objects in contact slide or roll relative to each other. Depending on the nature of the system, friction can arise due to dry contact (Coulomb friction), fluid shear (viscous friction), or internal forces (internal friction). The tangential force required to initiate motion (static friction force) is greater than the tangential force required to maintain relative motion (kinetic friction force). Friction is a system response rather than a material property.

Friction control in the presence of ultrasonic oscillations has been reported in the literature. One way of reducing friction is by superimposition of longitudinal or perpendicular vibrations on the macroscopic motion between two solids.[1] Coulomb's friction law has been shown to be applicable while modeling contact mechanics in ultrasonic applications.[2] Energy considerations have been used to show that a significant reduction in friction can be attained with little additional energy applied to the system. Recently, it was demonstrated using numerical analysis that Dahl's friction model is more appropriate while modeling friction reduction in the presence of superimposed longitudinal vibrations.[3]

The application of ultrasonic vibrations to actively modulate friction forces can be utilized in various vehicle systems (e.g., gear trains, sliding door/window mechanisms, seat belt systems, engine cylinders, brake systems, etc.), which often present contradicting requirements between sliding velocity, tangential and normal forces, and heat dissipation due to friction effects. Superposition of high-frequency vibrations on low-frequency disturbances or dither control has been proposed for suppressing squeal in automotive brake systems.[4,5] It has been shown that there is a reduction in friction between the brake pad and rotor due to the application of a normal dither signal.[6] Introduction of normal dither signals causes a small reduction in the braking torque (<2 percent).[4]

Further author information: (Send correspondence to M.J.D.)
M.J.D.: E-mail: dapino.1@osu.edu, Telephone: 1 614 688 3689
S.B.: E-mail: bharadwaj.4@osu.edu, Telephone: 1 614 247 7480

Industrial and Commercial Applications of Smart Structures Technologies 2010,
edited by M. Brett McMickell, Kevin M. Farinholt, Proc. of SPIE Vol. 7645,
76450P · © 2010 SPIE · CCC code: 0277-786X/10/$18 · doi: 10.1117/12.848914

Downloaded From: http://proceedings.spiedigitallibrary.org/ on 07/12/2017 Terms of Use: http://spiedigitallibrary.org/ss/termsofuse.aspx

Active or smart pads have been developed[7] which include embedded piezoelectric elements between the brake pad material and the metallic backing plate to generate a normal harmonic force. This force provides a small variation about the mean clamping force. Tangential dither influences the friction force due to its averaging effect whereas normal dither changes the mean friction coefficient.

This paper aims to experimentally characterize the behavior of sliding friction in seat belts in the presence of ultrasonic vibrations superimposed normal to the direction of motion. By precisely controlling the seat belt force during a crash event, superior restraint can be achieved relative to existing systems which are designed as a compromise for various occupants and loading conditions. Proof-of-concept experiments are presented which utilize a commercial ultrasonic welder and an apparatus for creating controlled relative motion between the welder tip and a seat belt webbing. Analytical modeling using LuGre friction is presented which characterizes the parametric dependence of friction reduction on system settings in the presence of ultrasonic vibrations.

2. EXPERIMENTS

In an automotive seat belt system, the maximum tension load experienced by a seat belt during a crash is around 700 N at the interface of the D-ring and seat belt. Previous experiments[9] confirm that the effect of friction reduction decreases with increasing load and thus there is a need for high power ultrasonics to achieve a given amount of friction reduction. A 2.5 kW Dukane 220 ultrasonic plastic welder is utilized in order to experimentally determine the performance limits and mechanics of a seat belt system subjected to macroscopic sliding motion and superimposed out-of-plane ultrasonic vibrations. These vibrations modulate the normal contact deflection at the interface in a sinusoidal manner about an average value. This reduces the effective area of contact and hence the friction force. The friction force is measured during motion of the seat belt with and without ultrasonic vibrations and the percentage decrease is quantified. By changing the normal load, the effect of load on the friction reduction is determined. The duration of the ultrasonics ON time and the amplitude of the vibrations are varied and their effect on friction reduction is quantified.

2.1 Experimental Setup

The experimental setup shown in Figure 1 consists of an automotive seat belt retractor assembly connected to a load cell. The load cell is fixed to a double-acting pneumatic actuator using a connector bracket. The load cell measures the pull force exerted by the actuator on the belt. The pneumatic actuator retracts at a steady speed of 0.025 m/s for a distance of 12 inches. The Dukane welder can generate ultrasonic vibrations up to an amplitude of 85 μm at an operating frequency of 20 kHz. A pneumatic cylinder connected to the waveguide inside of the welder is capable of applying normal loads up to 1500 N. The load is calculated by multiplying the air pressure by the area of the cylinder inside the ram. In these experiments, a normal load of up to 670 N is applied. Table 1 shows specifications of the Dukane welder.

Table 1. Specifications of Dukane 220 ultrasonic plastic welder.

Operating frequency	20,000 Hz
Maximum normal (static) load	1500 N
Power	2.5 kW
Horn material	Heat treated steel
Maximum amplitude	85 μm
Half wavelength	12.7 cm (5 in)
Air pressure for pneumatic cylinder	96.5-103.4 kPa (14-45 psi)

Downloaded From: http://proceedings.spiedigitallibrary.org/ on 07/12/2017 Terms of Use: http://spiedigitallibrary.org/ss/termsofuse.aspx

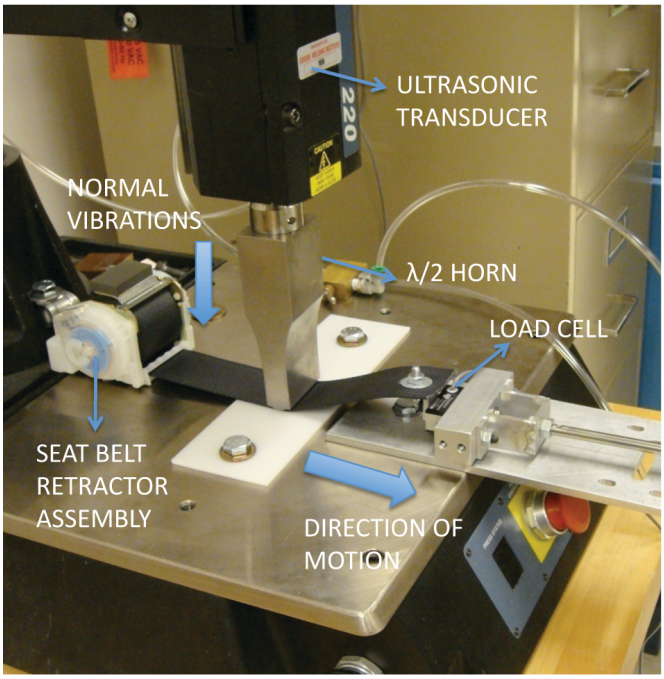

Figure 1. Experimental setup consisting of an ultrasonic welder, seat belt webbing, pneumatic actuator, and load cell.

2.2 Results

Experiments are presented which illustrate how the system responds under various ON times, static loads, and ultrasonic vibration amplitudes.

2.2.1 Effect of Ultrasonic Vibrations ON Time

Four measurements are presented in Figure 2 at 0.5, 1, 2, and 2.5 s duration of ultrasonic ON time. The friction force measured by the load cell decays and subsequently increases with the same constant slope for all four cases. This slope is dictated by the speed at which the pneumatic actuator pulls the seat belt webbing. This speed is constant as the pneumatic pressure was held constant throughout the tests. For the 0.5 and 1 second ON time, not enough time is allowed for the webbing to reach steady-state velocity, hence the amount of friction force reduction is limited by the ON time. For the 2 and 2.5 second cases, the webbing reaches steady-state velocity and the amount of friction reduction is maximum, near 60%. No further improvement in friction reduction is expected for longer ON times as the effectiveness of the friction reduction is, in these two cases, limited by the available ultrasonic power rather than the ON time.

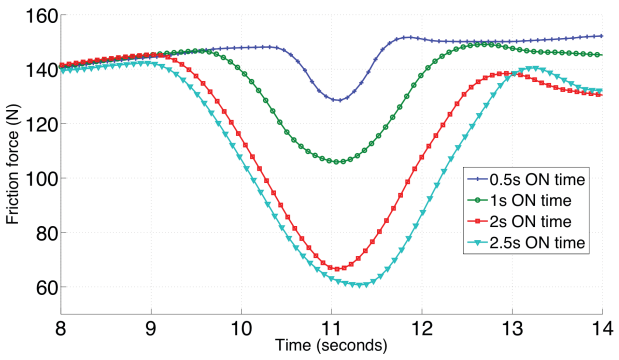

Figure 2. Effect of duration of ultrasonics ON time on friction reduction (670 N static load, 50% amplitude).

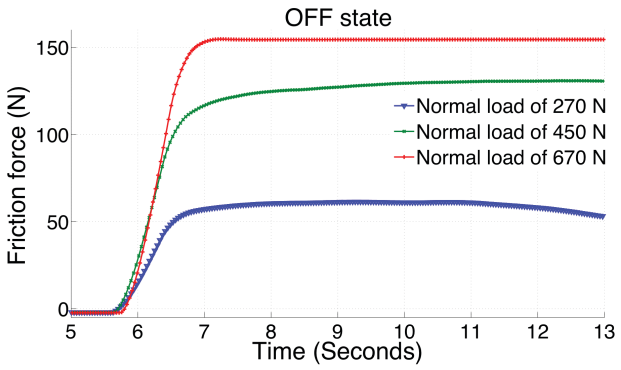

Figure 3. Effect of static normal load on friction force in the OFF state.

Downloaded From: http://proceedings.spiedigitallibrary.org/ on 07/12/2017 Terms of Use: http://spiedigitallibrary.org/ss/termsofuse.aspx

2.2.2 Effect of Static Load and Vibration Amplitude on Friction Force

Figure 3 shows the time trace of friction force at static loads of 270, 450, and 670 N and no applied ultrasonic vibrations. Due to the different normal loads and associated tangential forces acting on the webbing, the air pressure into the pneumatic cylinder was adjusted so that the belt moved at a constant speed of 25 mm/s. Flow valves restrict the air flow into the cylinder and as a result, there is a delay due to the air filling time. This is resolved by removing the valves and controlling the air pressure at the source. Ultrasonic vibrations are applied at 50% and 70% of the maximum amplitude capacity of the Dukane welder (85 μm). The results are shown in Figure 4. The vibration amplitude correlates nonlinearly to the ultrasonic energy fed into the system. As the normal load increases, more ultrasonic energy is required to achieve a given reduction in friction force.

Figure 5 compares the friction force in the OFF state, 50% amplitude, and 70% amplitude at a static load of 450 N. The degree of friction reduction increases with increasing amplitude and associated ultrasonic energy. There is no significant change in the friction force between the 50% and 70% vibration amplitudes. The rate of change of friction force changes as a result of the change in tangential force acting on the belt. At higher vibration amplitude, the belt tends to slide faster and hence the rate at which the friction force decays or increases is higher.

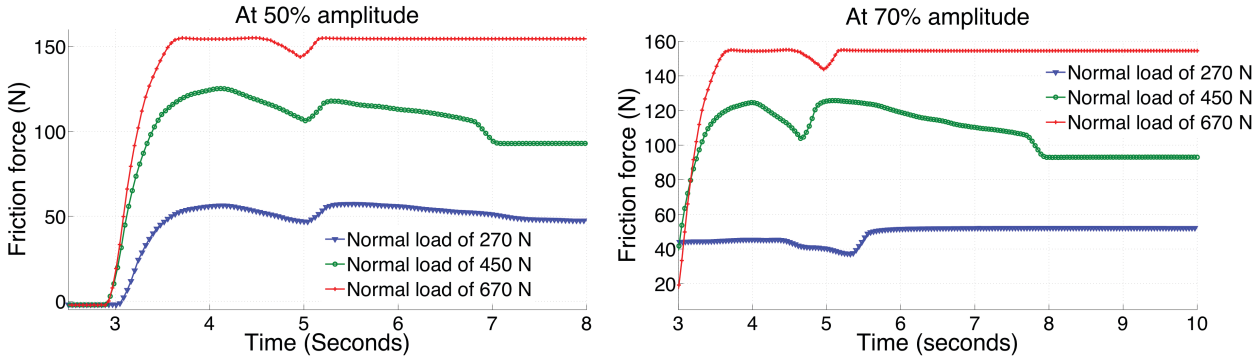

Figure 4. Effect of load on friction force reduction, (a) 50% vibration amplitude and (b) 70% amplitude.

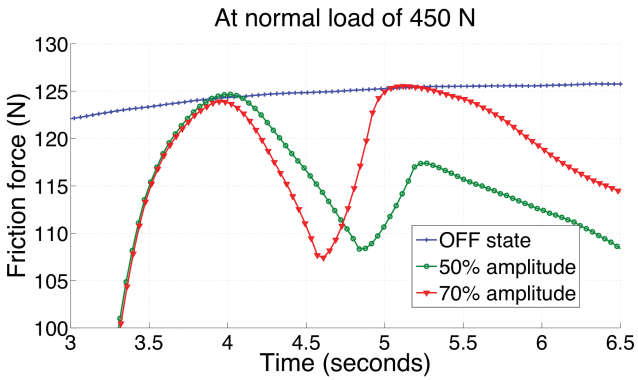

Figure 5. Effect of vibration amplitude on friction reduction at a static load of 450 N.

3. ANALYTICAL MODELING

3.1 LuGre Model

Classical friction models include different components, each addressing certain properties of the friction force.[2] The Coulomb friction model has been used to derive analytical expressions relating the friction reduction ratio with the velocity ratio. Representation of the discontinuity at zero slip velocity has been a concern, hence more sophisticated friction models classified as state variable friction laws that use differential equations are used to describe the friction force. These models are hysteretic in nature and have internal dynamics. The Dahl friction

Downloaded From: http://proceedings.spiedigitallibrary.org/ on 07/12/2017 Terms of Use: http://spiedigitallibrary.org/ss/termsofuse.aspx

model is one such example where the contact asperities are modeled as micro-springs. The effective contact stiffness is taken into consideration and the product of the stiffness and the elastic displacement of the asperities gives rise to the friction force. Researchers at the Lund Institute of Technology, Sweden, and the University of Grenoble, France developed the LuGre friction model. Here, the contact asperities are modeled as bristles that deflect like a spring when subject to a tangential force (Figure 6). This model incorporates the effect of surfaces being pushed apart by a layer of lubricant and describes the Stribeck effect. This model includes many of the features of friction behavior observed in experiments.

In the LuGre friction model the contact interface between two solids is represented by spring-like bristles. The deflection of the bristles gives rise to friction force. The deflections of each bristle are random and different; the average bristle deflection can be defined by a first order differential equation,

$$\dot{Z} = V - \frac{|V|}{G(V)} Z, \tag{1}$$

where V is the relative velocity and $G(V)$ is a positive function defined as

$$G(V) = \frac{1}{K_t}\{F_c + (F_s - F_c)e^{-(V/V_s)^2}\}. \tag{2}$$

Here, K_t is the tangential stiffness of the bristles, F_s is the static friction force, F_c is the kinetic friction force, and V_s is the Stribeck velocity. The LuGre friction force is defined as

$$F_L(V, Z) = \ K_t Z + \ \sigma_1 \dot{Z} + \ \sigma_2 V, \tag{3}$$

where σ_1 is the damping coefficient of the bristles and σ_2 accounts for viscous friction between the sliding objects.

For piezoelectrically driven systems at low velocities, viscous friction and the Stribeck effect can be ignored. Then, the LuGre friction reduces to

$$\dot{F}_L(V, Z) = \ K_t\{V - \frac{|V|}{G(V)} Z\}. \tag{4}$$

Since the Stribeck velocity is very small compared to the relative velocity, the function $G(V)$ reduces to F_c/K_t. Combination of (1)-(4) gives the following expression for the LuGre friction,

$$\dot{F}_L(V, Z) = \ K_t V\{1 - \frac{sgn(V)}{F_C} F_L\} = \dot{F}_D. \tag{5}$$

This relation implies that the LuGre friction reduces to the Dahl friction in the absence of internal damping and Stribeck effect.

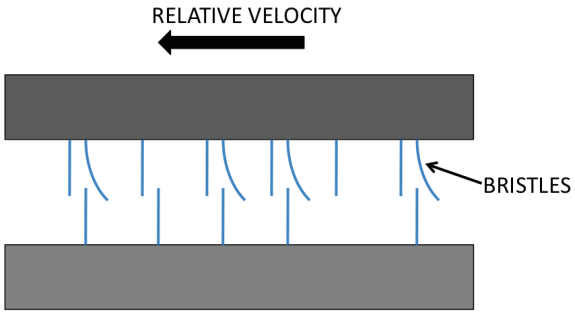

Figure 6. Schematic of the LuGre friction model.

Downloaded From: http://proceedings.spiedigitallibrary.org/ on 07/12/2017 Terms of Use: http://spiedigitallibrary.org/ss/termsofuse.aspx

3.2 System Model

The assumption of negligible internal damping is justified since damping is minimal in piezoelectric systems typically utilized in ultrasonic transduction. Additionally, since the range of displacements is very small, viscous friction does not affect the system dynamics. Thus, an ultrasonic transducer can be modeled as a single degree-of-freedom system with Dahl friction acting at the sliding interface and subjected to a harmonic excitation, as shown in Figure 7.

The governing equation of motion for the SDOF vibratory system with Dahl friction is

$$m\ddot{x} + K_s x = F_e \cos\omega t - F_D(t), \tag{6}$$

where m is the mass of the sliding body, K_s is the system stiffness, F_e is the piezo control force generated due to an applied voltage, and ω is the excitation frequency. From (5), the Dahl friction force has the form

$$\dot{F}_D(t) = K_t(V_t - \dot{x})\left\{1 - \frac{sgn(V_t - \dot{x})}{\mu mg} F_D(t)\right\} \tag{7}$$

where K_t is the tangential contact stiffness, μ is the coefficient of friction, and $V = V_t - \dot{x}$ is the relative velocity.

The friction force is approximated by numerical integration using the explicit fixed time step solver, fourth-order Runge-Kutta method. The nonlinearity due to the signum function dictates piecewise integration.

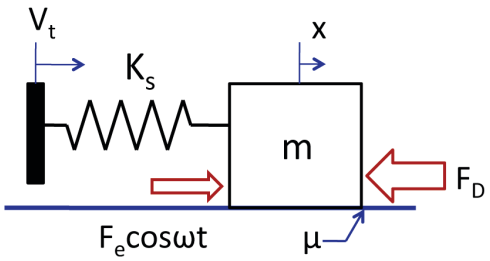

Figure 7. Single degree-of-freedom model of an ultrasonic transducer.

3.3 Model Parameters

Table 2 shows the system parameters employed in the calculations presented in Section 3.6.

Table 2. Parameters used for model calculations.

Parameter	Value
Mass, m	0.02 kg
System stiffness, K_s	133 x 10^6 N/m
Excitation frequency, ω	2π x 60,000 rad/s
Piezo control force, F_e	0 to 1920 N
Tangential stiffness of bristles, K_t	0.056 x 10^6 N/m
Coefficient of friction, μ	0.1
Solver	Fourth order Runge – Kutta method
Time step size	1.667 x 10^{-8} s (Fixed)

Downloaded From: http://proceedings.spiedigitallibrary.org/ on 07/12/2017 Terms of Use: http://spiedigitallibrary.org/ss/termsofuse.aspx

3.4 Dimensionless Ratios

Three dimensionless ratios are defined in order to quantify the effectiveness of the friction reduction system:

$$\text{Friction ratio} = \frac{\text{Friction force with ultrasonics ON}}{\text{Friction force with ultrasonics OFF}}, \tag{8}$$

$$\text{Power dissipation ratio} = \frac{\text{Friction power dissipated with ultrasonics ON}}{\text{Friction power dissipated with ultrasonics OFF}}, \tag{9}$$

$$\text{Velocity ratio} = \frac{\text{Macroscopic sliding velocity}}{\text{Velocity of ultrasonic waves}}. \tag{10}$$

For the system to be effective in reducing friction, the friction ratio must be as low as possible and the power dissipation ratio must be as high as possible. The velocity ratio must be kept below 1 for the system to be effective. The macroscopic sliding velocity is assumed to be a fixed system property, hence the frequency of ultrasonic vibrations must be sufficiently high in order for the velocity ratio to be less than 1. It is emphasized that while piezoelectric materials can operate at extremely high frequencies, their 2nd-order response yields increasingly low vibration amplitudes as the drive frequency increases.

3.5 Energy Considerations

Considering the system in Figure 7 without ultrasonic inputs, the velocity V_t is caused by an external force F_i. The mechanical energy over a period T is

$$E_{i,OFF} = F_i V_t T. \tag{11}$$

This energy is used as kinetic energy and the rest is dissipated,

$$F_i V_t T = \frac{1}{2} m {V_t}^2 + F_n V_t T. \tag{12}$$

where F_n is the intrinsic friction force in the absence of ultrasonic vibrations.

When the ultrasonic vibrations are switched on, the total input energy includes the mechanical input and the piezoelectric input,

$$E_{i,ON} = F_i V_t T + \int_0^T F_e(t)\dot{x}(t)dt, \tag{13}$$

where F_e is the piezoelectric excitation force. Combination of (12) and (13) gives

$$E_{i,ON} = \frac{1}{2} m {V_t}^2 + F_n V_t T + \int_0^T F_e(t)\dot{x}(t)dt. \tag{14}$$

This energy is converted to kinetic energy and spring potential energy, and the remaining is dissipated due to friction. The average kinetic energy during time T is

$$\begin{aligned} E_{ku} &= \frac{1}{T}\int_0^T \frac{1}{2} m (V_{rel}(t))^2 dt \\ &= \frac{1}{T}\int_0^T \frac{1}{2} m (V_t - \dot{x}(t))^2 dt. \end{aligned} \tag{15}$$

The average energy stored in the spring during time T is

$$E_{pu} = \frac{1}{T}\int_0^T \frac{1}{2} K_S (x(t))^2 dt. \tag{16}$$

Downloaded From: http://proceedings.spiedigitallibrary.org/ on 07/12/2017 Terms of Use: http://spiedigitallibrary.org/ss/termsofuse.aspx

The energy dissipated by friction force F_f during time T is

$$E_{fu} = \int_0^T F_f(t)(V_t - \dot{x}(t))dt. \tag{17}$$

Combination of (14)–(17) gives

$$\begin{aligned} \frac{1}{2}mV_t{}^2 + F_nV_tT + \int_0^T F_e(t)\dot{x}(t)dt = \frac{1}{T}\int_0^T \frac{1}{2}m(V_t - \dot{x}(t))^2dt + \frac{1}{T}\int_0^T \frac{1}{2}K_S(x(t))^2dt \\ + \int_0^T F_f(t)(V_t - \dot{x}(t))dt, \end{aligned} \tag{18}$$

$$\begin{aligned} F_nV_tT + \int_0^T F_e(t)\dot{x}(t)dt = \frac{1}{T}\int_0^T \frac{1}{2}m(\dot{x}(t))^2dt - \frac{1}{T}\int_0^T mV_t\dot{x}(t)dt \\ + \frac{1}{T}\int_0^T \frac{1}{2}K_S(x(t))^2dt + \int_0^T F_f(t)(V_t - \dot{x}(t))dt. \end{aligned} \tag{19}$$

With the definitions

$$E_{su} = \frac{1}{T}\int_0^T \frac{1}{2}m(\dot{x}(t))^2dt - \frac{1}{T}\int_0^T mV_t\dot{x}(t)dt + \frac{1}{T}\int_0^T \frac{1}{2}K_S(x(t))^2dt, \tag{20}$$

$$E_{iu} = \int_0^T F_e(t)\dot{x}(t)dt, \tag{21}$$

equation (19) yields an expression relating the input, internal, and dissipation energies

$$1 + \frac{E_{iu}}{E_f} = \frac{E_{su}}{E_f} + \frac{E_{fu}}{E_f}, \tag{22}$$

or

$$\frac{E_{fu}}{E_f} = 1 + \frac{E_{iu}}{E_f} - \frac{E_{su}}{E_f}, \tag{23}$$

in which $E_f = F_n\, V_t\, T$ is the energy dissipated due to friction with ultrasonic vibrations OFF, E_{iu} is the ultrasonic energy input into the system, and E_{su} is the system's internal energy (kinetic and potential). This expression can be written in terms of energy per unit time, or power P,

$$\frac{P_{fu}}{P_f} = 1 + \frac{P_{iu}}{P_f} - \frac{P_{su}}{P_f}, \tag{24}$$

Thus, the power dissipation ratio is given by

$$\phi_{ru} = 1 + \phi_{iu} - \phi_{su}, \tag{25}$$

where ϕ_{iu} is the ratio of the ultrasonic input power to the friction power dissipated with ultrasonic vibrations OFF and ϕ_{su} is the ratio of the power used by the system to the friction power dissipated with ultrasonic vibrations OFF. Physically, ϕ_{iu} represents the input power supplied to the system and ϕ_{su} represents the power consumed by the system in the form of potential and kinetic energy.

3.6 Effect of System Parameters on Friction Control

Relations (6) and (7) quantify the effect of system parameters on friction control. These parameters are mass, system stiffness, contact stiffness, piezoelectric control force, relative velocity, and coefficient of friction. The effect of load, velocity ratio and tangential stiffness[3] have been analyzed using Coulomb and Dahl equations. The effect of system dynamics on friction control is incorporated in this research. The velocity, displacement, friction force and power are not pure sinusoids as proposed by the Coulomb and Dahl models due to the effect of the natural frequency of the system. The calculations presented here correspond to a chosen set of parameters (Table 2) which are based on existing experimental and computational data presented by Leus and Gutowsky.[3]

Downloaded From: http://proceedings.spiedigitallibrary.org/ on 07/12/2017 Terms of Use: http://spiedigitallibrary.org/ss/termsofuse.aspx

3.6.1 Effect of Control Force

In a typical ultrasonic system, the control force is generated by piezoelectric elements when excited with a voltage. The relationship between the force generated and the applied voltage is assumed linear. This control force acts as an external excitation to a SDOF model at a given ultrasonic frequency. Figure 8(a) shows the effect of control force on the friction ratio. An increase in control force decreases the friction ratio. With higher control force, the velocity of vibration increases, which in turns decreases the velocity ratio. The power dissipation ratio correlates to the amount of input power required to obtain a desired velocity ratio and corresponding friction ratio. At velocity ratios at or above 1, the ultrasonic vibrations have no effect relative to the case when no ultrasonic vibrations are applied (Figure 8(b)). At low velocity ratios, high friction power is dissipated with ultrasonic vibrations ON. The higher the control force, the higher the dissipated power will be. As the control force is increased, the term P_{iu} increases. Thus, the power dissipation ratio increases with increasing control force.

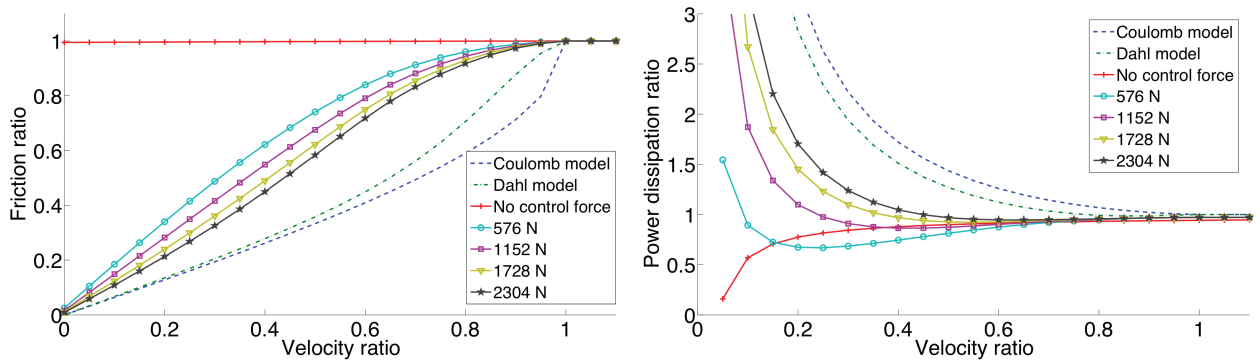

Figure 8. Effect of control force on (a) friction ratio vs. velocity ratio and (b) power dissipation ratio vs. velocity ratio.

3.6.2 Effect of Coefficient of Friction

The coefficient of friction determines the resistance offered to the sliding and vibratory motion of the mass. When the coefficient of friction is low, friction reduction is achieved more easily than when it is high. Figure 9(a) shows that the friction reduction is less effective as the friction coefficient increases. Power P_f is affected by the value of the friction coefficient. A high coefficient of friction implies a lower ϕ_{iu} and ϕ_{su}. As a result, the power dissipation ratio decreases with an increase in friction coefficient as shown in Figure 9(b).

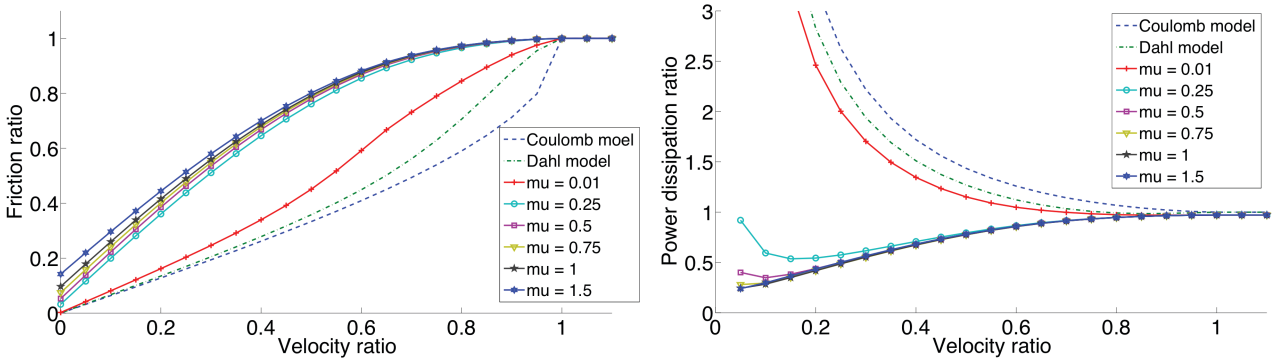

Figure 9. Effect of coefficient of friction on (a) friction ratio vs. velocity ratio and (b) power dissipation ratio vs. velocity ratio.

3.6.3 Effect of Mass Loading

An increase in mass load makes the friction reduction system less effective. Figure 10(a) shows that the friction ratio curve begins to flatten as load increases. This implies that for a given control force, the maximum possible

Downloaded From: http://proceedings.spiedigitallibrary.org/ on 07/12/2017 Terms of Use: http://spiedigitallibrary.org/ss/termsofuse.aspx

friction reduction is limited by the mass of the sliding body. An increase in normal load increases the friction force and leads to higher required ultrasonic energy. In Figure 10(b), the power dissipation ratio decreases as mass loading increases. The system energy increases, implying that at low velocity ratios, the power dissipated with ultrasonic vibrations is very low. The potential energy in the spring is much smaller in magnitude compared to the input energy. The effect of mass is significant in ϕ_{su}, which increases with increasing load.

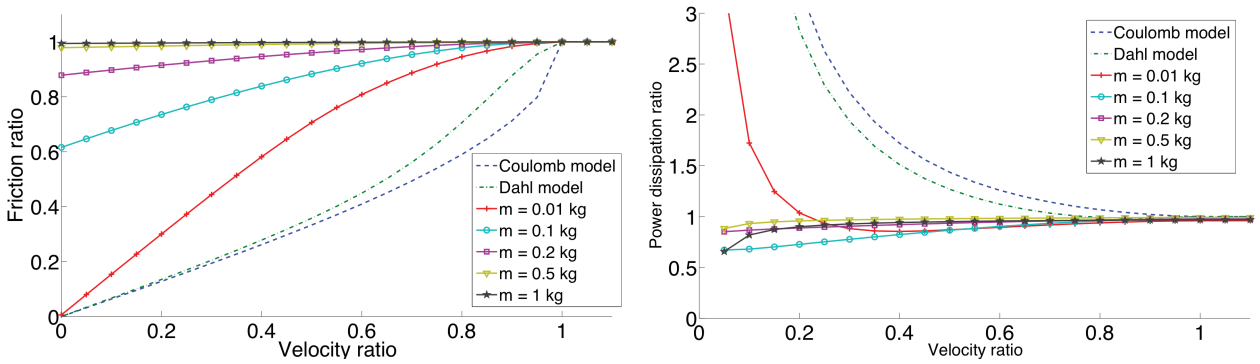

Figure 10. Effect of load on (a) friction ratio vs. velocity ratio and (b) power dissipation ratio vs. velocity ratio.

3.6.4 Effect of System Stiffness

The Coulomb model and Dahl models do not take the system stiffness into consideration. These analyses are based on assuming an infinitely stiff spring to which a mass is connected. In practice, the amount of friction reduction depends on system compliance. When the excitation frequency matches the system natural frequency, the displacement and hence the velocity of vibration increase. The velocity ratio therefore decreases, which in turn lowers the friction ratio (Figure 11(a)). At higher vibration velocities, the power dissipation due to friction is also high. For lower values of K_S, the power dissipation ratio is not significantly affected (Figure 11(b)). Thus, it is desirable to operate systems at their natural frequency to maximize the effect of friction reduction.

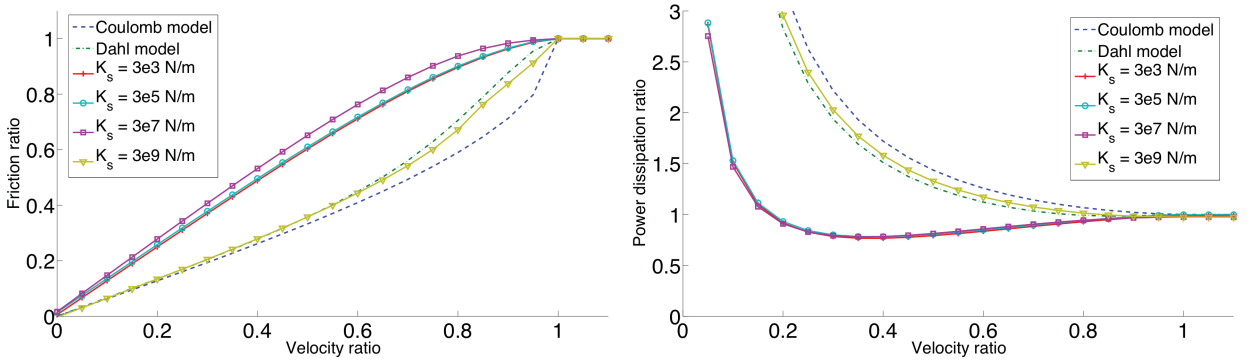

Figure 11. Effect of system stiffness on (a) friction ratio vs. velocity ratio and (b) power dissipation ratio vs. velocity ratio.

4. SUMMARY

This study experimentally demonstrates that ultrasonic vibrations superimposed normal to the macroscopic motion of a sliding seat belt can reduce friction at the interface. The extent of friction reduction depends on the velocity, load, vibration amplitude and duration. The effect is more pronounced for low velocities and normal loads. At higher loads, the friction force increases proportionally and the effect of friction reduction decreases.

The data shows that a friction reduction of up to 58% is achieved at a normal load of 670 N. This imposes a limit on the range of loads and speeds that allow for effective operation of the friction control system. Friction

Downloaded From: http://proceedings.spiedigitallibrary.org/ on 07/12/2017 Terms of Use: http://spiedigitallibrary.org/ss/termsofuse.aspx

behavior in the case of seat belt interfaces is complex. It is strongly dependent on the temperature, normal load and coefficient of friction. At high velocities, it is expected that local temperatures would rise due to friction heat dissipation in addition to heat energy generated by ultrasonic vibrations.

Based on the analytical model simulations, several conclusions are drawn. For maximum effectiveness in friction reduction, the excitation force must be as high as possible. This implies higher ultrasonic input power. The intrinsic coefficient of friction must be as low as possible. The operating frequency, if set to the natural frequency of the system, leads to greater friction reduction. The design of ultrasonic lubrication systems for friction control may be based on these parameters.

5. ACKNOWLEDGMENTS

We are grateful to the member organizations of the Smart Vehicle Concepts Center (www.SmartVehicleCenter.org) and the National Science Foundation Industry/University Cooperative Research Centers program (www.nsf.gov/eng/iip/iucrc) for providing financial support.

REFERENCES

[1] W. Littmann, H. Storck, and J. Wallaschek, "Sliding friction in the presence of ultrasonic oscillations: superposition of longitudinal oscillations," *Archive of Applied Mechanics,* 71, pp. 549-554 (2001).

[2] W. Littmann, H. Storck, and J. Wallaschek, "Reduction in friction using piezoelectrically excited ultrasonic vibrations," SPIEs 8th international Symposium on Smart Structures and Materials, Vol. 4331, pp. 302-311 (2001).

[3] M. Leus and P. Gutowski, "Analysis of longitudinal tangential contact vibration effect on friction force using Coulomb and Dahl models," *Journal of Theoretical and Applied Mechanics*, 46, pp. 171-184 (2008).

[4] J. Badertscher, K. Cunefare, and A. Ferri, "Braking impact of normal dither signals," *Journal of Vibration and Acoustics*, Vol. 129, pp. 18-23 (2007).

[5] M. Neubauer and R Oleskiewicz, "Brake squeal control with shunted piezoceramics efficient modeling and experiments," Proceedings of IMechE, Vol. 222, Part D: J. of Automotive Engineering, 592, pp. 1141-1151 (2008).

[6] K. Cunefare, and A. Graf, "Experimental active control of automotive disc brake rotor squeal using dither," *Journal of Sound and Vibration*, 250(4), pp. 579-590 (2002).

[7] P. Hagedorn, and U. von Wagner, "Smart pads: a new tool for the suppression of brake squeal?," Proceedings of XXIV μKolloquium, B. Breuer (Ed.), VDI-Bericht, Vol. 575 (2003).

[8] M. Michaux, A. Ferri, and K. Cunefare, "Effect of tangential dither signal on friction induced oscillations in an SDOF model," *Journal of Computational and Nonlinear Dynamics,* 2, pp. 201-210 (2007).

[9] S. Bharadwaj and M. J. Dapino, "Effect of load on active friction control using ultrasonic vibrations," Proceedings SPIE Smart Structures/NDE, Paper 7290-15 (2009).

[10] C.C. Tsai and C.H. Tseng, "The effect of friction reduction in the presence of in-plane vibrations," *Archive of Applied Mechanics,* 75, pp. 164-176 (2005).

Downloaded From: http://proceedings.spiedigitallibrary.org/ on 07/12/2017 Terms of Use: http://spiedigitallibrary.org/ss/termsofuse.aspx